Energy Conversion and Management: X 29 (2026) 101563

Contents lists available at ScienceDirect

Energy Conversion and Management: X

journal homepage: www.sciencedirect.com/journal/energy-conversion-and-management-x

Experimental evaluation of zeolite 13X and activated carbon as adsorbents in a carbon capture system for ICE exhaust gases

Alexander García Mariaca [a,d,*], Eva Llera Sastresa [b], Francisco Moreno [c], Uriel Fernando Carreno Sayago [d]

[a] Energy and CO_2 Group, Department of Mechanical Engineering, Aragon Institute of Engineering Research (I3A), University of Zaragoza, Zaragoza 50018, Spain
[b] Energy and CO_2 Group, Department of Mechanical Engineering and CIRCE Research Institute, University of Zaragoza, María de Luna s/n, Zaragoza 50018, Spain
[c] Energy and CO_2 Group, Department of Mechanical Engineering, University of Zaragoza, Zaragoza, Spain
[d] Faculty of Engineering and Basic Sciences, Fundación Universitaria los Libertadores, Bogotá 111221, Colombia

ARTICLE INFO

Keywords:
Carbon capture and storage
Internal combustion engine
Activated carbon
Zeolite 13X
Temperature swing adsorption

ABSTRACT

Given the urgent need to mitigate climate change, reducing CO_2 emissions produced by internal combustion engines (ICEs) remains a critical challenge in the transport sector. Onboard carbon capture (CC) systems have emerged as a promising alternative, attracting growing research interest in recent years. However, most studies are limited to simulations, with experimental evidence still scarce. Based on the above, this study experimentally evaluates zeolite 13X (Z13) and activated carbon (AC) as adsorbents for CO_2 capture in ICEs. For this purpose, an adsorption-based CC system was integrated into the exhaust duct of an ICE operating under partial loads and at two engine speeds. The experimental data were subsequently employed to develop a simulation case study aimed at performing an energy assessment of a carbon capture and storage (CCS) system based on temperature swing adsorption. The results show that the adsorbent Z13 demonstrated a 13 % higher CO_2 adsorption capacity and a 33 % longer capture duration than AC, though average carbon capture rates (CCR) remained moderate (25 % for Z13 and 16 % for AC). The case study results showed that the carbon capture and storage (CCS) system with Z13 achieves a maximum CCR of up to 37 %, an energy penalty of approximately 30 % of the engine's power output and an average energy consumption for CO_2 capture of 3900 kJ/kgCO_2. Conversely, the CCS system with AC did not provide suitable CCR or energy performance under any scenario. The case study also demonstrates that the CCS system has a better performance when the engine is operated at medium or higher loads.

1. Introduction

Meeting the 2050 emission reduction targets constitutes a fundamental global challenge that requires the active involvement of all productive sectors. Without such efforts, global warming will drastically alter human activities due to the societal impacts driven by climate change. For this reason, all technologies that reduce CO_2 emissions must continue to be explored for potential applications across the different industrial sectors.

However, key sectors such as industry and transport will continue to emit CO_2 during the energy transition, because they have applications where electrification is not yet practical in the short to medium term. In this vein, carbon capture, storage (CCS), and utilisation (CCSU) technologies have emerged as promising methods for use in these sectors, thereby mitigating their CO_2 emissions.

Specifically, the transport sector will continue to depend heavily on internal combustion engines (ICEs), which are among the main contributors to global net CO_2 emissions (approximately 23 % in 2022 [1]) due to their substantial reliance on fossil fuels for operation. As a result, in recent years, a growing body of research has focused on evaluating CCS systems in applications powered by ICE (trucks and ships), mainly assessing their energy, technical, and techno-economic feasibility [2]. In this way, the researchers aim to establish the potential of this technology to achieve decarbonisation in this sector.

In the maritime sector, whose objective is to reduce CO_2 emissions by at least 20 % by 2030 and 70 % by 2040 compared to 2008 [3], research has focused on CO_2 capture in post-combustion, with amine absorption

* Corresponding author at: Energy and CO_2 Group, Department of Mechanical Engineering, Aragon Institute of Engineering Research (I3A), University of Zaragoza, Zaragoza 50018, Spain.
E-mail addresses: alexander.garcia@unizar.es (A.G. Mariaca), ellera@unizar.es (E.L. Sastresa), fmoreno@unizar.es (F. Moreno), ufcarrenos@libertadores.edu.co (U.F. Carreno Sayago).

https://doi.org/10.1016/j.ecmx.2026.101563
Received 24 May 2025; Received in revised form 15 October 2025; Accepted 13 January 2026
Available online 14 January 2026

Nomenclature

AC	Activated carbon
cap	capture
CC	Carbon capture
CCR	Carbon capture rate
CCS	Carbon capture system
com	compressor
cool	Cooling
EG	Exhaust gases
EGT	Exhaust gases thermocouple
HC	Hydrocarbons
ICE	Internal combustion engine
PPP	Percentage of power penalty
reg	regeneration
RH	Relative humidity
sor	adsorbent
T	Temperature
TSA	Temperature swing adsorption
vac	vacuum
Z13	Zeolite 13X
ΔHads	Adsorption Heat
ΔT	Temperature difference
cp	Specific heat
$\dot{E}$	Energy
$\dot{m}$	mass flow
q	Loading capacity
$\dot{Q}$	Heat
$\dot{Q}_{sen}$	Sensitivity heat
$\dot{Q}_{des}$	Desorption heat
$\dot{W}$	Power

predominating, and to a lesser extent, adsorption. Regarding research on amine absorption [4–11], energy and techno-economic analyses have been made using MEA, DEA, and piperazine, achieving carbon capture rates (CCR) of up to 90 %. This approach is because maritime engines typically operate under quasi-stationary conditions, with relatively stable exhaust gas flow rates and CO_2 concentrations, similar to power plants. Moreover, the available space on vessels facilitates the installation of CCS units with limited impact on cargo capacity [12]. Regarding adsorption, a study investigated alumina-supported K_2CO_3 as a adsorbent material [13]. The authors indicated that this approach ensures safer operation, operational flexibility, and effective CO_2 capture at temperatures below 100 °C, achieving capture rates of up to 28 %. Finally, studies have also been conducted on pre-combustion capture technologies [14,15]. In these, a quasi-closed carbon cycle is proposed by integrating a reformer, where a fuel is converted into H_2 and CO_2. The H_2 is used as a fuel, and the CO_2 is cooled until liquefied and stored onboard, followed by its discharge at the harbour for its storage or utilisation.

On the other hand, in the context of road transport, research efforts have primarily focused on temperature swing adsorption (TSA) as a suitable technique for CO_2 capture [16–20]. These studies have examined the feasibility of carbon capture from both energy and economic perspectives, testing a variety of adsorbents, including Porous Polymer Networks (PPNs), Metal–Organic Frameworks (MOFs), zeolites, and activated carbon [21,22]. Additionally, these studies present a preliminary design of a CCS system operating with TSA, remarking that this design occupies only 6 % of the available volume of a bus [23,24]. Notably, they have also explored the integration of Organic Rankine Cycles (ORCs) as energy recovery systems to supply the additional power required during the CO_2 storage stage, mainly due to compression processes. The main findings indicate that achieving 100 % CCR is technically feasible, with an engine power penalty of less than 10 %. Among the adsorbents tested, MOF-74-Mg showed the best performance compared to its counterparts. However, techno-economic analyses indicate that implementation is not feasible unless the transport sector faces CO_2 emission rights costs exceeding 250 €/ton CO_2 [23,25].

Despite theoretical advances and optimistic projections, most studies presented previously have relied on computational simulations with assumptions that diverge from the operative reality of ICE. Although these approaches represent a preliminary step in technological development and feasibility assessment, they remain insufficient to approximate real-world applications.

In this vein, critical issues must be evaluated experimentally; for instance, the CCS system must be able to operate under highly transient engine operation, characterised by rapid accelerations, decelerations, and variable load conditions, which produce variations in the flow, species concentration, and temperature of the exhaust gases, without forgetting that the integration of a CCS will entail additional energy consumption, thereby reducing the power output produce by the ICE. According to the literature review, the authors agree that for the road transport sector, TSA seem to be the most suitable CO_2 capture technique for adapting to these conditions [26]. This is due to different reasons, among which is that the heat of adsorption is lower than that of absorption [27], so the waste heat of the exhaust gases can cover the thermal demand of regeneration of the adsorbent, and the other is that the TSA is a cyclical process; therefore, when these variations occur, the duration of the cycle could be adjusted to match the engine's operation, slowing it down or accelerating it, which would not dramatically affect the CCR [28,29]. However, to develop a fully functional CCS system operated by TSA, several key aspects must be examined experimentally. Among these, the choice of adsorbent for CO_2 capture is especially crucial, as it influences the volume, heat input, and cooling capacity needed by the CCS system.

In view of the knowledge gaps identified above, the objective of this paper is to experimentally assess the performance of two commercial adsorbents (activated carbon and zeolite 13X) operating in a carbon capture (CC) system coupled to an internal combustion engine under two engine speeds and varying load conditions. Complementarily, a simulation case study developed in ASPEN+, and informed by experimental data, is conducted to examine key design factors of the CCS system, such as the regeneration heat and cooling requirements of the TSA cycle, the compressor power consumption for CO_2 storage, and the overall energy penalty imposed on the engine. Furthermore, the experimental tests and simulations enable the evaluation of key variables, such as maximum CCR, capture time, adsorbent behaviour in the presence of other pollutants, engine performance penalties, energy demand for CO_2 capture, and the potential of utilising exhaust gas waste heat to supply the regeneration process. The results obtained, both experimentally and through the case study, not only strengthen the scientific knowledge base on carbon capture in transportation but also provide concrete data that could support further technological development. This, in turn, would contribute to accelerating the transition towards more sustainable transport systems aligned with global climate objectives.

2. Materials and methods

2.1. Bench test

The experimental setup employed a Lombardini 523 MPI spark ignition engine, the main technical specifications of which are detailed in Table 1. The engine was mounted on a test bench and mechanically

Table 1
Engine specifications.

Property	Value
Number of cylinders	2
Bore × Stroke	72 × 62 mm
Compression ratio	10.7:1
Valves per cylinder	2
Fuel delivery system	Electronic indirect fuel injection

coupled to a Tecner E315 dynamometer, which enables the precise measurement of rotational speed and load, with respective accuracies of ±5 rpm and ±0.5 Nm. The test bench is equipped with a volumetric liquid fuel flow meter specifically for gasoline consumption assessment. The intake air flow rate was determined using a Foxboro 823 differential pressure transmitter, which quantifies the pressure drop across a calibrated nozzle in accordance with the specifications outlined in the British Standard.

The composition of the exhaust gases was measured using a non-dispersive infrared analyser for CO_2, a flame ionisation detector for hydrocarbons (HC), and a paramagnetic analyser for O_2, all manufactured by Signal Instruments, with measurement accuracies specified in Table 2. The equivalence ratio was directly monitored using a Bosch LSU 4.9 wideband lambda sensor installed in the engine's exhaust, controlled by a Tech Edge 3H1 unit. It is noteworthy that the test conditions (encompassing power output, fuel consumption, and pollutant emissions) as well as the accuracy of the measurement instruments complied with the protocols established by current European regulatory directives. Data acquisition from all sensors was carried out using software developed in LabVIEW. A schematic representation of the test bench configuration is provided in Fig. 1.

2.2. CC system device

The CC system employed is shown in Fig. 2. It was designed to operate with samples containing between 12 % and 15 % by mass of the total exhaust gases. The sample is extracted using a vacuum pump powered externally. Initially, the extracted gas passes through a vessel equipped with a calibrated orifice, which allows for the determination of the gas's mass flow rate. Subsequently, the sample flows through two counterflow heat exchangers arranged in series to reduce the gas temperature to its dew point. The cooled gas stream then enters a cyclone, where the condensed water is separated, ensuring that the exhaust gases reaching the vessel containing the adsorbent are completely dry.

This design aims to prevent the adsorbent from becoming contaminated with moisture. Finally, after passing through the adsorbent, the composition of the exhaust gases is measured in the gas analyser. The gas sensing system is equipped with a set of valves that enables operation in two configurations: in the first one, the raw exhaust gases from the engine is blocked, and measurement of the gases treated by the CC system device is enabled; In the second configuration, direct analysis of the engine exhaust gases is allowed, while the gas stream that trough the CC system device is vented to the atmosphere.

Thermocouples, pressure gauges and flow meters are installed to register data to assess the CO_2 capture rate, the adsorbent's loading capacity and saturation time, the energy consumption of the adsorption process, the heat required for water condensation, and the behaviour of other emissions (such as CO and NO_x) when interacting with the adsorbent material.

Table 2
Gas analyser Accuracy.

Gas	Accuracy
CO_2	±0.1 % (0–10 %) ±0.2 % (10–25 %)
HC	±1 ppm (0–100 ppm) ±4 ppm (100–400 ppm) ±10 ppm (400–1000 ppm) ±40 ppm (1000–4000 ppm)
O_2	±0.1 % (0–10 %) ±0.2 % (10–25 %)

2.3. Adsorbent selection

For the experimental tests, zeolite 13X supplied by Fisher Scientific (onwards Z13) and biomass-derived activated carbon supplied by Strem Chemicals (onwards AC) were selected. Z13 has a particle size of 3 mm and a spherical shape, and AC has a size between 3–5 mm and an irregular shape. The selection of these adsorbents is due to Z13 and AC sharing similar properties with other adsorbents [30–33]; their main disadvantage lies in the lower CO_2/N_2 selectivity compared to advanced adsorbents, such as MOFs or PPNs [31]. Additionally, under humid conditions (such as those present in ICE exhaust gases), PPNs, Z13, and AC can operate effectively, albeit with a reduced CO_2 capture capacity [34], whereas MOFs are unstable under these conditions [35]. Finally, Z13 and AC are highlighted because they are commercially available adsorbents, in contrast to PPNs, whose large-scale production remains limited [36].

Fig. 3a and 3b present the SEM images of the adsorbents employed in the experimental tests. Z13 sample exhibits a heterogeneous, granular microstructure composed of aggregates of well-defined crystalline particles, predominantly cubic in morphology. The surface is rough and fractured, consistent with a high BET surface area exceeding 750 m2/g [37]. In contrast, the AC sample shows a relatively smooth surface, suggesting that most of its porosity is microporous and internal, in agreement with a BET surface area of approximately 500 m2/g, derived from biomass sources [38]. Bright spots observed on the surface correspond to inorganic residues or ash particles embedded within the carbon matrix. The adsorbent's properties are shown in Table 3.

2.4. Experimental and simulation procedures

The test preparation begins with the determination of each adsorbent's bulk density. As the carbon capture will be performed in a fixed bed, a 1000 cc vessel is loaded with 400 g of adsorbent, intentionally avoiding complete filling to minimise pressure drops and loading losses in the system. Two distinct engine operating conditions were selected for the experimental evaluation: the first at 2700 rpm with a torque of 5 Nm, and the second at 3600 rpm with a torque of 13 Nm. These operating regimes were chosen because the engine reaches its maximum torque within this RPM range. Table 4 shows the test name, the adsorbent bulk density obtained, the adsorbent mass and the engine load used in the tests.

The test begins by operating the engine at the preselected rotational speed until it reaches a stable operating temperature, defined as an engine oil temperature of 90 °C. Once this condition is achieved, engine performance and emission measurements are conducted for a duration of one minute, in accordance with ISO 8178-1:2020. Subsequently, the vacuum pump is activated to allow a sample of exhaust gases to pass through the CC system. Once the CO_2 concentration measured at the outlet of the CC system reaches the same value as that recorded in the engine exhaust duct, the valve assembly is reversed, thereby concluding the measurement process (see Fig. 2). The flow rate of the exhaust gas sample is determined in a vessel equipped with a calibrated orifice plate, which enables the quantification of the volumetric flow rate by measuring the pressure drop generated across the orifice. Each test is repeated three times for each engine and adsorbent condition.

In addition to determining the behaviour of Z13 and AC as carbon capture adsorbents and the behaviour of other emissions (such as CO and NO_x) upon contact with the adsorbent material, the most important objective of this study is to assess the energy consumption associated with the adsorption process. Regarding the heat requirement for water

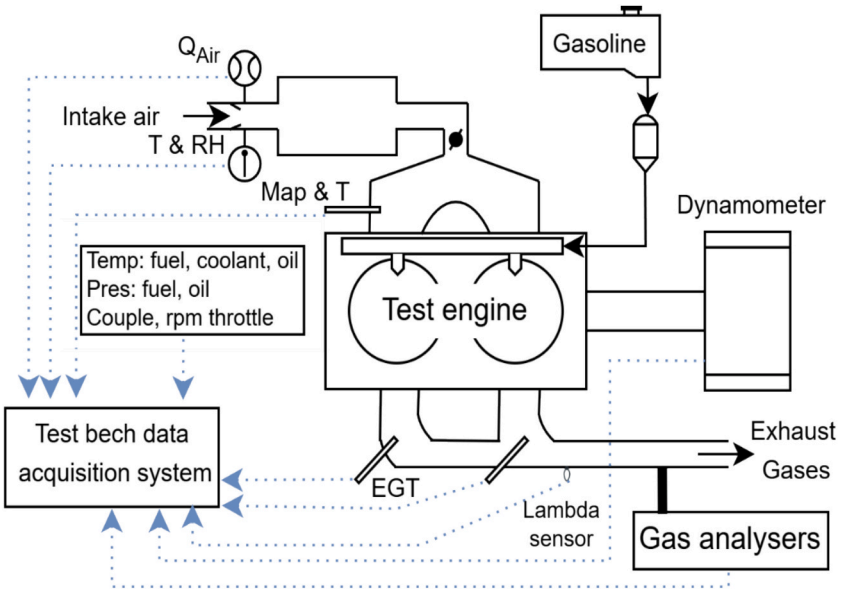

Fig. 1. Schematic diagram of the test bench.

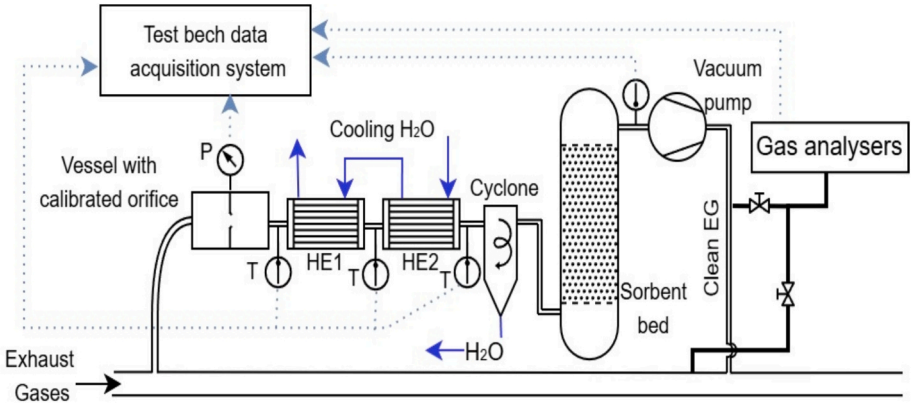

Fig. 2. Schematic diagram of the carbon capture system.

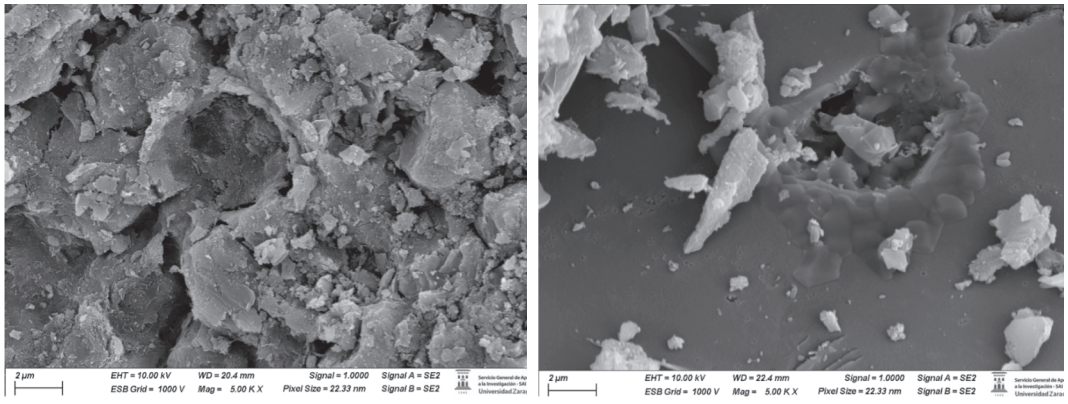

a) Zeolite 13X (Z13) b) Activated carbon (AC)

Fig. 3. SEM images at 2 μm of adsorbents utilised in the experimental tests.

condensation, certain calculations are necessary, including the determination of the molar and mass fractions of the exhaust gases on a wet basis, as well as the estimation of the mass flow rate of the exhaust gas sample. The latter is derived from differential pressure measurements taken in the vessel equipped with a calibrated orifice, located upstream of the heat exchangers (see Fig. 2).

To ensure the reliability and repeatability of the engine variable measurements under the established speed and engine load conditions,

Table 3
Adsorbent properties.

Property	Z13	AC	Ref.
Adsorption Heat (ΔH_{ads}) [kJ/mol$_{CO2}$]	−49.72	−25	[31,39]
Selectivity CO_2/N_2	17.46	11	[31,39]
Specific Heat (c_p) [kJ/kgK]	1.07	1.062	[31,39]
Loading Capacity (q) [kg$_{CO2}$/kg$_{sor}$]	0.176	0.132	[31,39]
BET surface area [m^2/g]	786	485	[37,38]
Pore volume [cm^3/g]	0.35	0.3	[37,38,40]

Table 4
Engine conditions and adsorbent mass used in the experimental tests.

Tests names	Torque [Nm]	Engine power [kW]	Mass adsorbent [g]	Density [kg/m^3]
Z13-2700	5	1.4	419.5 ± 3	666.7
Z13-3600	13	4.9	417.8 ± 2	
AC-2700	5	1.4	405.4 ± 1	449.4
AC-3600	13	4.9	405.1 ± 1	

A total of four experimental campaigns were carried out, each consisting of three repetitions, to ensure the stability and consistency of the recorded parameters. In addition, CO_2 capture experiments were conducted at a rate of one test per day, utilising a different adsorbent material for each test. The testing schedule was also varied across the campaigns to evaluate the potential impact of environmental conditions. Overall, these four campaigns, with their three repetitions, resulted in a total of twelve CO_2 capture tests. The gas analyser was calibrated daily to reduce measurement uncertainties. In total, twenty-four experimental tests were performed, yielding robust and reliable data for subsequent analysis.

Finally, to estimate the power required by the compressor to store CO_2 in its liquid state, simulations are carried out for each case using Aspen + software. In these simulations, an isentropic efficiency of 65 % is assumed for the compressor, a value widely reported in the scientific literature for this type of process [19], and a adsorbent regeneration efficiency of 100 % for CO_2 capture. Based on these results, the energy penalty associated with implementing the CCS system over the ICE is determined, as well as the total CO_2 energy consumption required by the CO_2 capture process. The properties of the adsorbents (Z13 and AC) used in the simulations are presented in Table 3.

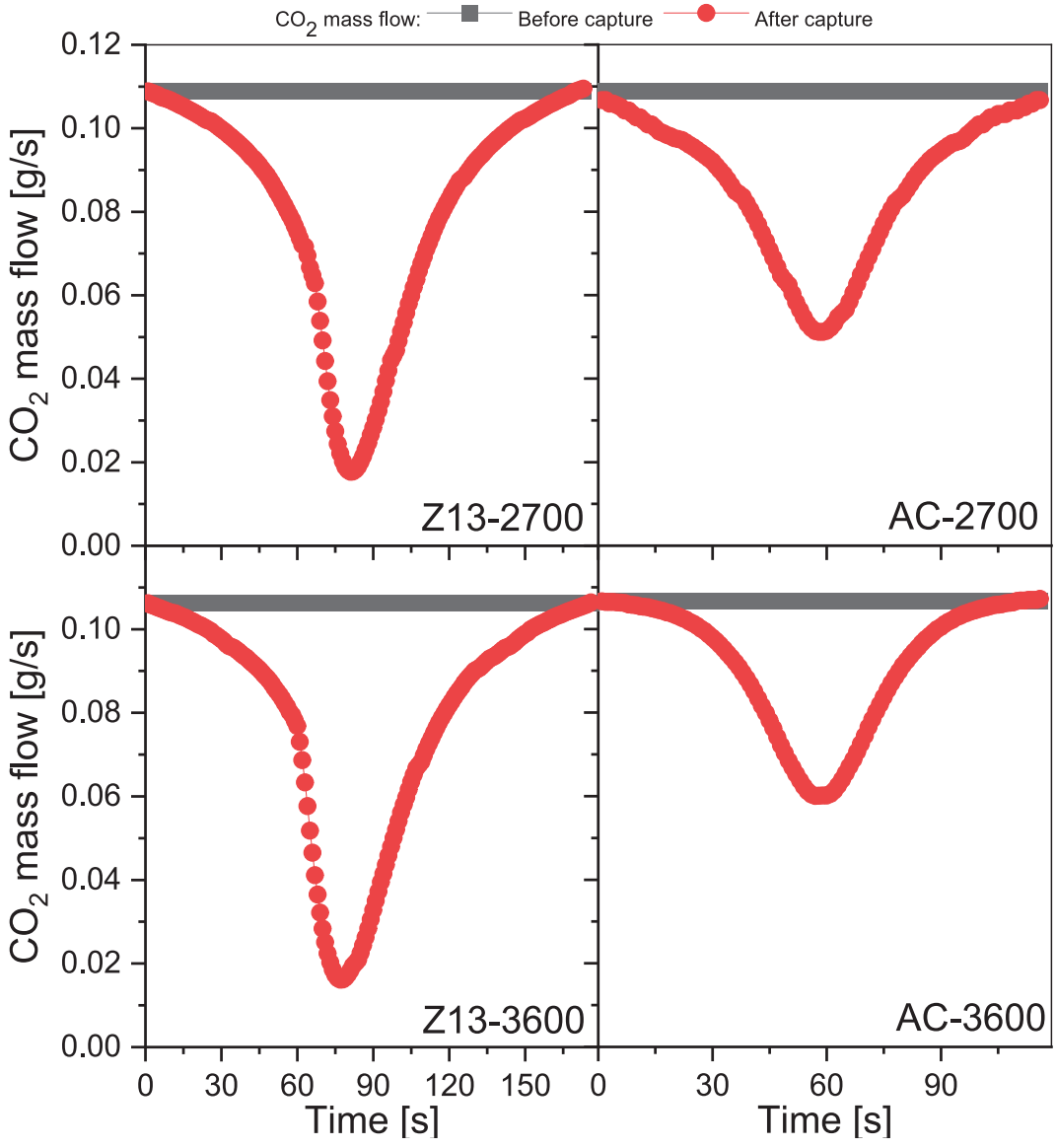

Fig. 4. CO_2 mass flow in the CC system operating with Z13 and AC at 2700 and 3600 rpm.

3. Results

3.1. Carbon capture rate and capture time

Fig. 4 illustrates the CO_2 mass flow rate at the outlet of the capture device during the experimental tests. Under both engine operating modes, a similar trend is observed regarding CO_2 capture behaviour and capture duration for each adsorbent evaluated. This consistency is attributed to the operation of the vacuum pump used for exhaust gas sampling, which maintains a constant extraction flow rate regardless of engine speed or torque. Consequently, the variations in capture performance are primarily associated with the intrinsic adsorption properties of the adsorbents, rather than fluctuations in the inlet flow to the CC system.

As shown in Fig. 5, the Z13 adsorbent demonstrates superior performance in CO_2 adsorption compared to AC, both in terms of capture efficiency and process duration. Specifically, Z13 achieves a more pronounced reduction in the CO_2 mass flow, reaching minimum values of around 0.02 g/s, whereas AC reduces the flow to approximately 0.06 g/s. This indicates a higher adsorption capacity for Z13. Moreover, the capture duration with Z13 is extended by approximately 60 s relative to AC, further confirming its better performance under the tested conditions.

Fig. 5 illustrates the net CCR obtained during the experimental tests. The CCR was calculated using Equation (1). As can be seen, the Z13 adsorbent outperforms AC under both engine operating conditions, achieving an average CCR of 25.3 %, compared to 16.5 % for AC. This performance difference is further highlighted in Fig. 6, which presents SEM images of the CO_2-saturated adsorbents. The images clearly show, at least on the surface, that Z13 retains a greater amount of CO_2 on its surface than AC, confirming its superior adsorption capacity and efficiency under the tested conditions.

$$CCR[\%] = \frac{\dot{m}_{CO_{2\_in}} - \dot{m}_{CO_{2\_out}}}{\dot{m}_{CO_{2\_in}}} \times 100 \quad (1)$$

This enhanced performance of Z13 is attributed to its higher adsorption capacity, which is approximately 37 % greater than that of AC, and its better structural parameters compared to the AC, since Z13 has a 62.1 % and a 16.7 % more BET surface area and pore volume than AC, respectively (see Table 3). Therefore, it is consistent that Z13 exhibits a higher CO_2 uptake due to its greater number of active adsorption sites and a larger internal space available compared to AC. Moreover, the presence of cations within the crystalline framework of Z13 promotes strong electrostatic interactions with CO_2 molecules [41], thereby enhancing its affinity relative to the predominantly non-polar surface of AC [42,43].

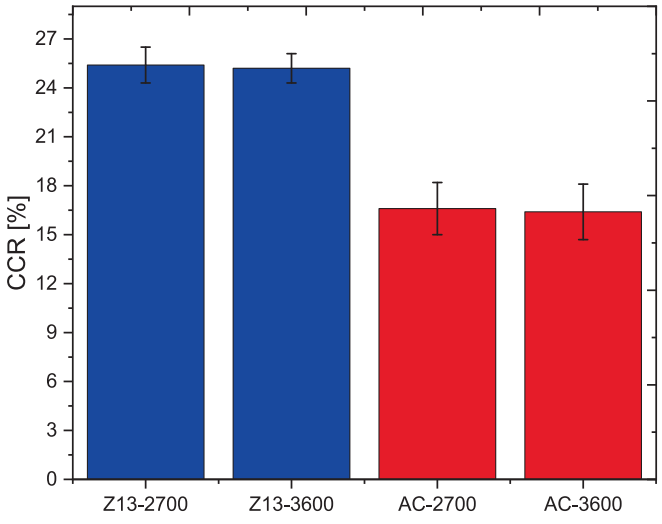

Fig. 5. CCR obtained in the experimental test.

Finally, the morphological characteristics play a crucial role in CO_2 uptake. While AC particles exhibit an irregular shape, Z13 particles possess a uniform spherical geometry, which facilitates a more homogeneous flow of exhaust gases through the adsorption bed, thereby improving CO_2 adsorption [44,45]. Additionally, with the AC, the CO_2 loading could be affected because, as can be inferred from its selectivity value in Table 3, it tends to exhibit a broader adsorption spectrum, retaining not only CO_2 but also other exhaust gas components [46]. This non-selective adsorption behaviour reduces the adequate capacity of AC for capturing CO_2.

Another factor that could influence the CCR of AC is the simultaneous absorption of CO_2 and H_2O. According to the literature, ACs exposed to moist atmospheres, such as flue gases, exhibit reduced CO_2 uptake [46], which has been attributed to kinetic effects in H_2O diffusion within the pores and to possible interactions between CO_2 and H_2O within the pore structure. On the other hand, Z13, according to the literature, does not show a reduction in CO_2 uptake in the presence of water [47]. This behaviour has been attributed to chemisorption facilitated by water, resulting in the formation of carbonates or bicarbonates.

3.2. Adsorption of other species in exhaust gases

The NOx and CO emissions measured after the CC system did not exhibit significant changes with any adsorbent. Both materials have a low CO/N_2 selectivity of approximately 1.3 and a limited loading capacity of 0.0112 kg kg_{CO}/kg_{sor} [48,49], which is about one order of magnitude lower than the values reported for Z13 and AC (see Table 3). For the case of NOx, the adsorption of NOx on AC is only significant under high oxygen concentrations [50], as the ICE operated under stoichiometric conditions, the NOx uptake was negligible. For Z13, no changes were also observed in NOx measurements after the CC system, which can be attributed to its intrinsic physical properties, as NO exhibits a very low selectivity compared with CO_2, with a value of 7.5×10^{-7} kg_{CO}/kg_{sor} [51].

The only emission that showed a notable variation was HC. The HC concentrations obtained during the experimental tests are presented in Fig. 7. As can be seen, both adsorbents significantly decreased the levels of HC, with a decline of almost 60 % for AC and 70 % for Z13 relative to their original concentration. These results align with the expected behaviour, as AC and Z13 are widely recognised for their effectiveness in HC adsorption due to their high BET surface area and pore volume (see Table 3), leading to high values of loading capacity for CH_4/N_2, which, according to the literature, is approximately 3.4 [52]. Notably, both adsorbents maintained their adsorption capacity for hydrocarbons (HC) even when saturated with CO_2. This suggests a preferential adsorption of HC over CO_2, arising from the non-polarity and small size of HC, which enable stronger interactions with the adsorbent surface, even in the presence of CO_2, a phenomenon known as competitive adsorption [53].

3.3. CO_2 loading capacity of adsorbents

One of the most critical variables in assessing the performance of adsorbent materials is their CO_2 loading capacity (q), defined as the amount of CO_2 adsorbed per unit mass of adsorbent. In this study, the experimental values obtained were 0.0136 and 0.0061 g_{CO2}/g_{sor} for Z13 and AC, respectively (Table 5). These values are significantly lower (less than 90 %) than those reported in the literature, where loading capacities of 0.176 g_{CO2}/g_{sor} for Z13 and 0.132 g_{CO2}/g_{sor} for AC have been documented [31,39].

The primary reason for this discrepancy lies in the experimental conditions under which the tests were conducted. Most research studies employ synthetic gas mixtures under highly controlled conditions, free of moisture and trace species such as HC, CO, among others. In contrast, the present study is based on real exhaust gases emitted from an ICE.

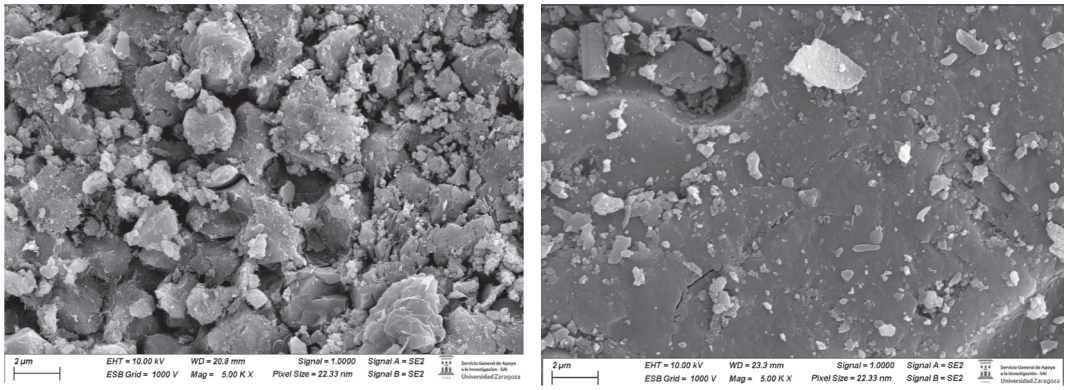

a) Zeolite 13X (Z13) b) Activated carbon (AC)

Fig. 6. SEM images at 2 μm of saturated adsorbents utilised in the experimental tests.

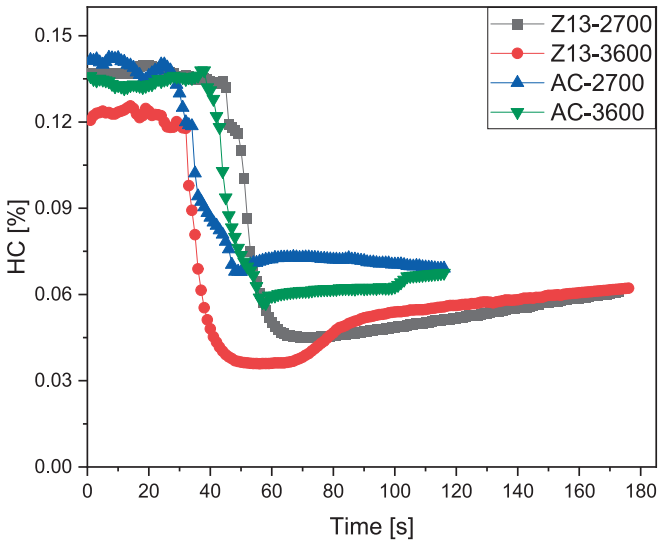

Fig. 7. HC reduction in the experimental test.

Consequently, the complex composition of the exhaust stream significantly influences the adsorption behaviour of the adsorbents.

The limited CO_2 loading observed for AC is primarily attributed to its higher affinity for water and hydrocarbons, and to a lesser extent, for NOx and CO, which also influence its adsorption performance. Additionally, the BET surface area of the biomass-derived AC used in this study is lower than that of conventional activated carbons (>1000 m2/g [54]), further restricting CO_2 uptake. Z13 exhibits similar behaviour, with the distinction that it maintains a relatively stable CO_2 adsorption capacity under humid conditions, according to the literature [44,45]. Hence, and despite the suitable condition of the Z13 for CO_2 uptake in humid gases, the main reason for the reduced CO_2 capture in both adsorbents is the high water content in the exhaust gases, which promotes preferential water adsorption over CO_2. This is supported by measurements of condensed water collected in the cyclone before the CC system, which correspond to approximately 50 % of the water produced during stoichiometric combustion by the ICE, as shown in Table 5.

3.4. Regeneration and cooling heat

Temperature Swing Adsorption (TSA) involves four main stages: (i) heating of the adsorbent (sensitive heat, Equation (2); (ii) desorption of CO_2 (desorption heat, Equation (3); (iii) cooling of the adsorbent (sensitive heat without CO_2); and (iv) CO_2 capture (adsorption heat). The first two stages are collectively referred to as the regeneration heat ($\dot{Q}_{reg}$), as represented in Equation (4), while the latter two can be grouped as the cooling heat ($\dot{Q}_{cool}$). According to the literature, the optimal desorption temperature is approximately 150 °C [31]. Therefore, for the purpose of calculations, a temperature difference (ΔT) of 120 °C was considered, since experimental tests showed that the exhaust gas cooling temperature at the outlet of the heat exchangers was 30 °C (Equation (2). The desorption heat, defined as the energy required for the release or capture of CO_2 by the adsorbent, is obtained from the adsorbent desorption enthalpy (ΔH_{des}), as presented in Equation (3). Additionally, the heat content of the exhaust gases ($\dot{Q}_{EG}$) was calculated using Equation (5), where ΔT in this equation correspond to the temperature difference between the measured exhaust gas temperature at the engine outlet and the desorption temperature. The results obtained from this calculation are presented in Table 6.

$$\dot{Q}_{sen} = c_{p\_CO_2}\dot{m}_{CO_{2\_cap}}\Delta T + c_{p\_sor}\dot{m}_{sor}\Delta T \quad (2)$$

$$\dot{Q}_{des} = \dot{m}_{CO_{2\_cap}}\Delta H_{des} \quad (3)$$

$$\dot{Q}_{reg} = \dot{Q}_{sen} + \dot{Q}_{des} \quad (4)$$

Table 6
Heat of regeneration, cooling and exhaust gases.

Test	$\dot{Q}_{reg}$ [kW]	$\dot{Q}_{cool}$ [kW]	$\dot{Q}_{EG}$ [kW]
Z13-2700	−0.354	0.350	0.704
AC-2700	−0.467	0.465	0.681
Z13-3600	−0.344	0.341	0.725
AC-3600	−0.451	0.449	0.727

Table 5
Experimental values of CO_2 loading capacity for the evaluated adsorbents.

Test	Mass of CO_2 captured [g]	Adsorbent mass [g]	q [g_{CO2}/g_{sor}]	Mass of H_2O condensed [g]
Z13-2700	5.72	419.5	0.0136	2.75
AC-2700	2.47	405.4	0.0061	1.81
Z13-3600	5.62	417.8	0.0135	2.75
AC-3600	2.44	405.1	0.0060	1.82

$$\dot{Q}_{EG} = \dot{m}_{EG} c_{p\_EG} \Delta T \quad (5)$$

The results presented in the previous table indicate that the heat content of the exhaust gases in the case of Z13 is more than twice the amount required for adsorbent regeneration. For the AC adsorbent, the heat available in the exhaust gases exceeds the regeneration requirement by approximately 50 %. In both cases, therefore, the thermal energy contained in the exhaust gases is sufficient to meet the CO_2 desorption demand at the obtained capture rates. Furthermore, to meet the cooling requirement reported in Table 6, a volumetric airflow of approximately 0.06 m^3/s is needed for Z13 and 0.079 m^3/s for AC. These flow rates can be supplied by a standard fan, such as those commonly used in the radiator systems of ICE cooling circuits.

3.5. Percentage of power penalty on the engine and CCS energy consumption

To estimate the percentage of power penalty (PPP) of the CCS on the engine, it is necessary to calculate the parasitic loads, which are the sum of the powers of compression and vacuum. A simulation was conducted using the Aspen + software to determine the compression power ($\dot{W}_{com}$). In this simulation, a compressor with an isentropic efficiency of 65 % was considered [19]. Additionally, the selectivity of each adsorbent (Table 3) was taken into account to determine the nitrogen concentration in the final stream of captured CO_2, and thereby estimate the total pressure required for the CO_2 to reach liquefaction conditions, set at 75 bar and 29.3 °C. Once the compressor power requirement was obtained, the PPP imposed by the CO_2 capture system on the engine was calculated using Equation (6). The vacuum power ($\dot{W}_{Vac}$) measured in the experimental tests was 0.08 kW. The energy consumption of the CO_2 capture process is calculated using Equation (7). Table 7 shows the results obtained.

$$PPP = \frac{\dot{W}_{com} + \dot{W}_{Vac}}{\dot{W}_{ICE}} x100\% \quad (6)$$

$$\dot{E}_{cap} = \frac{\dot{W}_{com} + \dot{W}_{Vac}}{\dot{m}_{CO2}} \quad (7)$$

As shown in Table 7, the PPP under both ICE operating conditions is higher for the AC adsorbent than for Z13. This is attributed to the fact that the total pressure required to liquefy CO_2 with AC is 85.71 bar, compared to 81.75 bar for Z13. This means that the compressor requires more power to reach the pressure demanded by AC, resulting in higher values of PPP. Nevertheless, at 3600 rpm, a condition under which the ICE operates at higher load, the difference in PPP between the two adsorbents diminishes, with PPP values of 3.9 % for Z13 and 4 % for AC.

On the other hand, the average energy consumption obtained across all test conditions was approximately 1500 kJ/kgCO_2, regardless of the engine's operating condition. This is explained by the fact that the compression power between tests remained practically unchanged, resulting in minimal variations in the results. It is worth noting that the average value obtained in these experimental tests is lower than that reported for capture systems based on amine-scrubbing, where the average energy consumption is on the order of 2500 kJ/kgCO_2 [55,56].

Table 7
Power compression, PPP and energy consumption of the CC system.

Test	$\dot{W}_{com}$ [kW]	PPP [%]	$\dot{E}_{cap}$ [kJ/kgCO_2]
Z13-2700	0.113	13.6 %	1477.5
AC-2700	0.117	13.9 %	1511.5
Z13-3600	0.113	3.9 %	1508.3
AC-3600	0.117	4.0 %	1543.0

3.6. Critical analysis of the design of a TSA-based CC system

A critical assessment of the implementation of CC systems in mobile sources reveals that their development and deployment still face several challenges. The most significant factors include the regeneration and cooling times of the systems, as well as determining the optimal number of beds required for operation (all of them related to the device's dimensioning). A study was found in the literature where it was conducted to dimension a TSA device for mobile applications [23]. According to this research, a bed with a diameter of 8 cm and a length of 1 m has heating and cooling times of approximately 360 s, which is in line with the times found in other research, indicating that these times take around 400 s [57]. Regarding the number of fixed-bed requirements, studies indicate that at least three beds are necessary to accomplish the four phases (capture, heating, desorption and cooling) of the TSA process [58]. In this manner, the TSA device will comprise a series of fixed beds operating in parallel, as illustrated in Fig. 8.

In the literature, it has been proposed that this type of system could be addressed either by means of a rotating adsorber wheel [21,22] or by a complex system of pipes, pumps, valves, and other auxiliary components [23]. While both proposals are interesting to address in the design of the CC system, they still need to be validated experimentally and provide data such as the volume required for its installation, the back-pressure generated in the engine, adsorbent loading and unloading cycles, use of materials that allow rapid heating and cooling (high levels of thermal fatigue) and other key parameters.

4. Case study and sensitivity analysis

In the initial case study, a CCR of 100 % and a capture time of 200 s are assumed as starting conditions to quantify the mass of adsorbent required under each engine operating condition and to verify whether the heat contained in the exhaust gases is sufficient to meet the thermal demand associated with adsorbent heating and desorption processes. According to the results presented in Table 8, the required adsorbent mass in both engine conditions with Z13 is 55 % less than with AC. These calculations consider the loading capacity values for the adsorbents obtained in the experimental tests (Table 5). Therefore, given the lower loading capacity of AC, the CCS requires a greater mass of adsorbent compared to Z13.

The results for the sensible heat, desorption heat, and the heat contained in the exhaust gases are presented in Table 9. As shown, the sensible heat demand is significantly higher, being 9 times greater than the desorption heat in the case of Z13 and 57 times greater in the case of AC. When comparing the sum of these two heats with the heat contained in the exhaust gases, it becomes clear that the available heat is

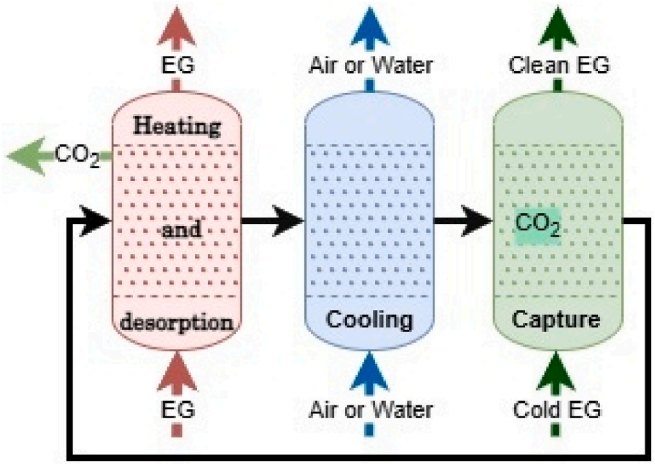

Fig. 8. Minimum adsorbent fixed beds required in TSA.

Table 8
Adsorbent mass obtained at 100% of CCR.

Test	$\dot{m}_{EG}$ [kg/h]	$\dot{m}_{CO2}$ [kg/h]	Adsorbent mass [kg]
Z13-2700	19.04	2.94	10.80
AC-2700			24.09
Z13-3600	24.40	3.77	13.85
AC-3600			30.88

Table 9
Sensible and desorption heat, and the heat contained in the exhaust gases at 100% of CCR.

Test	$\dot{Q}_{sen}$ [kW]	$\dot{Q}_{der}$ [kW]	$\dot{Q}_{EG}$ [kW]
Z13-2700	8.10	−0.92	3.59
AC-2700	26.55	−0.46	3.44
Z13-3600	10.21	−1.18	4.89
AC-3600	34.03	−0.59	4.90

insufficient to meet the thermal requirements for adsorbent regeneration under a 100 % CCR and a capture time of 200 s.

Two sensitivity analyses were conducted to evaluate the performance of the CO_2 capture system. In the first analysis, the CCR was held constant at 100 % while the capture time was varied. In the second analysis, the procedure was reversed: the capture time was maintained constant at 200 s, and the CCR was varied. These analyses allowed the determination of the minimum operating time and CCR where the regeneration heat required by the adsorbent can be supplied exclusively by the engine's exhaust gases. Fig. 9 presents the results obtained from both sensitivity analyses.

In Fig. 9, it is shown that the regeneration heat can be entirely supplied by the energy contained in the exhaust gases when the CO_2 capture system operates for a maximum of 60 s using adsorbent Z13, and for 20 s when using AC. When compared with the experimentally obtained times (see Fig. 4), the regeneration period that can be covered with the waste heat of the exhaust gases for AC is extremely short, which prevents a CCS system using this adsorbent from reaching a satisfactory CCR. In contrast, with Z13, the waste heat of the exhaust gases can cover roughly half of the regeneration time, so that the CCR would be less affected. These results are entirely consistent with the outcomes of the second sensitivity analysis, where the maximum CCR achieved was, on average, 37 % for Z13 and 11.5 % for AC, under the established sensitivity analysis conditions. Based on these values, the PPP was calculated, as illustrated in Fig. 10. It can be seen that, when the engine operates at 2700 rpm, the average 88 %, while at 3600 rpm, it decreases to values close to 30 % for both adsorbents. This is entirely expected, as higher rpm operation of the engine generates more waste heat in the exhaust gases, which can be used to reduce the PPP regardless of the type of adsorbent used.

Fig. 11 shows the parasitic load associated with the operation of the CCS system and the overall energy consumption of the CO_2 capture process. As shown in this figure, when using AC, the energy consumption exceeds 11000 kJ/kgCO_2 under both engine operating conditions. This behaviour is attributed to higher parasitic loads, resulting from increased compressor and vacuum power demands (values detailed in Appendix A) necessary for the CCS system to capture 100 % of the emitted CO_2 by the engine. Conversely, when using Z13, the energy consumption under both engine conditions is approximately 3900 kJ/kg$_{CO2}$; this reduction regarding AC is primarily due to the greater mass of CO_2 captured with Z13. Nevertheless, the energy consumption

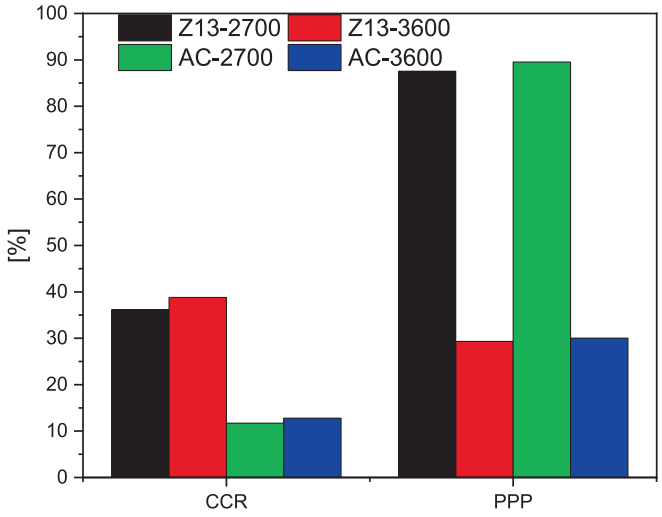

Fig. 10. CCR and PPP found in the case study.

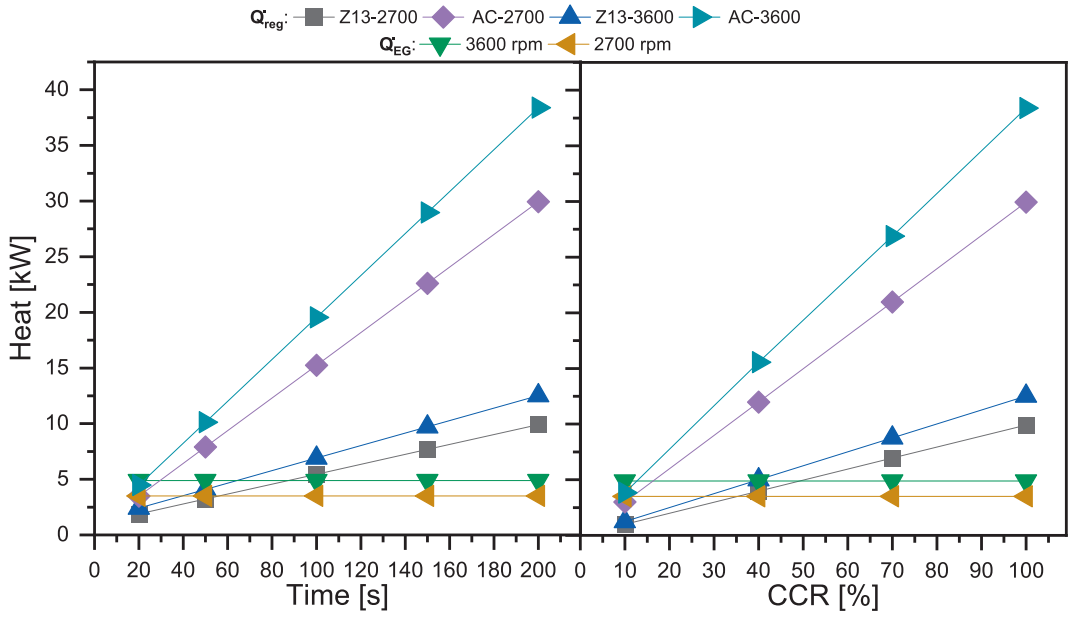

Fig. 9. Results of sensitivity analyses.

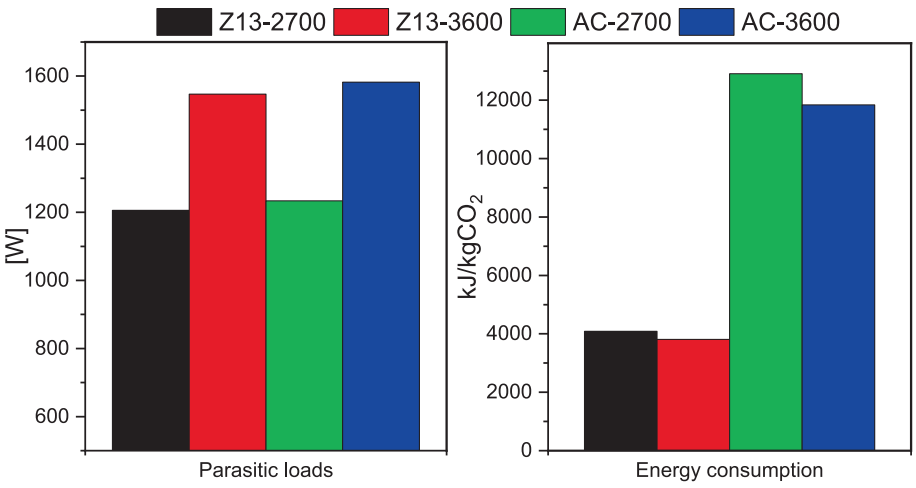

Fig. 11. Parasitic loads and energy consumption obtained in the case study.

obtained for both adsorbents under any engine operating condition remains considerably higher than the values typically reported in the literature [56].

5. Conclusions

This research work focused on the experimental evaluation of two commercial adsorbents (Z13 and AC) for CO_2 capture in mobile sources powered by ICE. Experimental tests were conducted on a CC system, and a case study, along with a sensitivity analysis of a CCS system operating with the TSA process, were developed, with the aim of identifying the energy requirements that condition the performance of these systems in mobile sources.

Based on the results obtained, it is concluded that Z13 exhibited significantly superior performance compared to AC under the evaluated conditions. Specifically, Z13 achieved a 13 % higher CCR and a more effective reduction of HC in the exhaust gases compared to AC. Moreover, CO_2 storage using Z13 resulted in lower PPP than AC. These findings position Z13 as a potential adsorbent for CO_2 capture in transport applications, pending further validation under dynamic, cyclic and long-term operating conditions. It should be noted, however, that these results are subject to experimental limitations, including the absence of a continuous operation strategy, the lack of implemented regeneration, simplified gas flow conditions, and the non-direct quantification of humidity, which may affect the generalisation of the findings.

The case study and sensitivity analysis revealed that the heat contained in the exhaust gases can only meet the thermal regeneration requirements for a maximum CCR of 37 % when using Z13 and 11.5 % when using AC. Furthermore, the analysis showed that when the engine operates at low loads and low rpm, the proposed CCS system is not viable from an energy perspective, as the PPP values and the energy consumption for CO_2 capture are significantly higher than those reported in the literature. However, this behaviour reverses as engine load and rpm increase, indicating a clear trend where the proposed CCS system enhances its energy performance as the engine's output power rises. This occurs because the compression and vacuum power requirements in the CCS system do not increase in proportion to the engine's power output.

On the other hand, based on the available heat in the exhaust gases, the integration of additional systems, such as organic Rankine cycles, to enhance the energy efficiency of the CCS system does not seem viable within the design proposed in this research, since all the heat available in the exhaust gases is already utilised for adsorbent regeneration.

Future research efforts should concentrate on optimising the design of the CC system to enhance both the CCR and the capture duration. This implies that future studies should focus on areas such as rapid adsorbent heating and cooling, employing vessels made of advanced materials capable of withstanding higher stresses induced by thermal fatigue; a comprehensive assessment of the energy requirements associated with modular system configurations; and the development and evaluation of adsorbents with enhanced CO_2 selectivity and moisture tolerance.

Additionally, comprehensive techno-economic studies and life cycle analyses should include estimates of capital and operational expenditures, as well as consider system weight and its impact on fuel consumption, the space required for installation, and the energy demand of the CC system. These factors are crucial for rigorously evaluating the economic feasibility and environmental impact of implementing CO_2 capture technologies in the transport sector. All these developments will be fundamental in ensuring that the transportation sector moves towards genuine sustainability in the short and medium term, in line with global climate change mitigation goals.

CRediT authorship contribution statement

Alexander García Mariaca: Writing – review & editing, Writing – original draft, Software, Methodology, Investigation, Formal analysis, Conceptualization. **Eva Llera Sastresa:** Writing – review & editing, Writing – original draft, Supervision, Resources, Investigation, Funding acquisition. **Francisco Moreno:** Visualization, Supervision, Methodology, Investigation, Formal analysis, Conceptualization. **Uriel Fernando Carreno Sayago:** .

Declaration of competing interest

The authors declare that they have no known competing financial interests or personal relationships that could have appeared to influence the work reported in this paper.

Acknowledgment

This paper is part of the R&D project PID2021-125137OB-I00, funded by MCIN/AEI/10.13039/501100011033/ and by “ERDF A way of making Europe“.

Appendix A. Compression and vacuum powers

Adsorbent	RPM	CCR [%]	Compression power [W]	Vacuum power [W]
Z13	2700	36,17	704,94	501
AC	2700	11,71	732,711	501
Z13	3600	38,78	903,733	643
AC	3600	12,77	939,32	643

Data availability

Data will be made available on request.

References

[1] International Energy Agency. Global CO_2 emissions by sector, 2019-2022 2023.
[2] García-Mariaca A, Llera-Sastresa E. Review on carbon capture in ICE driven transport. Energies (basel) 2021;14:6865. https://doi.org/10.3390/en14216865.
[3] International Maritime Organization. Energy efficiency and the reduction of GHG emissions from ships. 2023 IMO Strategy on Reduction of GHG Emissions from Ships 2023. https://www.imo.org/en/OurWork/Environment/Pages/2023-IMO-Strategy-on-Reduction-of-GHG-Emissions-from-Ships.aspx (accessed June 10, 2024).
[4] Feenstra M, Monteiro J, van den Akker JT, Abu-Zahra MRM, Gilling E, Goetheer E. Ship-based carbon capture onboard of diesel or LNG-fuelled ships. Int J Greenhouse Gas Control 2019;85:1–10. https://doi.org/10.1016/j.ijggc.2019.03.008.
[5] Ros JA, Skylogianni E, Doedée V, van den Akker JT, Vredeveldt AW, Linders MJG, et al. Advancements in ship-based carbon capture technology on board of LNG-fuelled ships. Int J Greenhouse Gas Control 2022;114:103575. https://doi.org/10.1016/J.IJGGC.2021.103575.
[6] Barrio M, Aspelund A, Weydahl T, Sandvik T, Wongraven L, Krogstad H, et al. Ship-based transport of CO_2. Greenhouse Gas Control Technologies 7. Elsevier 2005;53:1655–60. https://doi.org/10.1016/B978-008044704-9/50193-2.
[7] Fang S, Xu Y, Li Z, Ding Z, Liu L, Wang H. Optimal sizing of shipboard carbon capture system for maritime greenhouse emission control. IEEE Trans Ind Appl 2019;55:1. https://doi.org/10.1109/tia.2019.2934088.
[8] Luo X, Wang M. Study of solvent-based carbon capture for cargo ships through process modelling and simulation. Appl Energy 2017;195:402–13. https://doi.org/10.1016/j.apenergy.2017.03.027.
[9] Güler E, Ergin S. An investigation on the solvent based carbon capture and storage system by process modeling and comparisons with another carbon control methods for different ships. Int J Greenhouse Gas Control 2021;110:103438. https://doi.org/10.1016/J.IJGGC.2021.103438.
[10] Stec M, Tatarczuk A, Iluk T, Szul M. Reducing the energy efficiency design index for ships through a post-combustion carbon capture process. Int J Greenhouse Gas Control 2021;108. https://doi.org/10.1016/j.ijggc.2021.103333.
[11] Horvath S, Fasihi M, Breyer C. Techno-economic analysis of a decarbonized shipping sector: technology suggestions for a fleet in 2030 and 2040. Energy Convers Manag 2018;164:230–41. https://doi.org/10.1016/j.enconman.2018.02.098.
[12] Ahmed YA, Lazakis I, Mallouppas G. Advancements and challenges of onboard carbon capture and storage technologies for the maritime industry: a comprehensive review. Mar Syst Ocean Technol 2025;20:13. https://doi.org/10.1007/s40868-024-00161-w.
[13] Zhou P, Wang H. Carbon capture and storage – solidification and storage of carbon dioxide captured on ships. Ocean Eng 2014;91:172–80. https://doi.org/10.1016/j.oceaneng.2014.09.006.
[14] Chin Law L, Gkantonas S, Mengoni A, Mastorakos E. Onboard pre-combustion carbon capture with combined-cycle gas turbine power plant architectures for LNG-fuelled ship propulsion. Appl Therm Eng 2024;248:123294. https://doi.org/10.1016/j.applthermaleng.2024.123294.
[15] Malmgren E, Brynolf S, Fridell E, Grahn M, Andersson K. The environmental performance of a fossil-free ship propulsion system with onboard carbon capture – a life cycle assessment of the HyMethShip concept. Sustain Energy Fuels 2021;5:2753–70. https://doi.org/10.1039/d1se00105a.
[16] García Mariaca A, Llera E, Moreno F, Romeo LM. Energy efficiency evaluation of a mobile CCS-ORC system in operation with a heavy-duty engine. SSRN Electron J 2024. https://doi.org/10.2139/ssrn.5011978.
[17] Larkin C, Li K, Oliva F, García-García FR. Scaling up a hollow fibre adsorption unit for on-board CCS applications using a real gasoline engine exhaust. Chem Eng J 2024;497:154453. https://doi.org/10.1016/j.cej.2024.154453.
[18] Saravanan S, Kumar R. Experimental Investigations on CO_2 Recovery from Engine Exhaust Using Adsorption Technology. SAE Technical Paper 2019;2019-28–2577. https://doi.org/10.4271/2019-28-2577.Abstract.
[19] García-Mariaca A, Llera-Sastresa E, Moreno F. CO_2 capture feasibility by Temperature Swing Adsorption in heavy-duty engines from an energy perspective. Energy 2024;292:130511. https://doi.org/10.1016/j.energy.2024.130511.
[20] García-Mariaca A, Llera E. Dynamic CO_2 capture in a natural gas engine used in road freight transport. SSRN Electron J 2022. https://doi.org/10.2139/ssrn.4272013.
[21] Sharma S, Maréchal F. Carbon dioxide capture from internal combustion engine exhaust using temperature swing adsorption. Front Energy Res 2019;7:1–12. https://doi.org/10.3389/fenrg.2019.00143.
[22] García-Mariaca A, Llera-Sastresa E, Moreno F. Application of ORC to reduce the energy penalty of carbon capture in non-stationary ICE. Energy Convers Manag 2022;268:116029. https://doi.org/10.1016/J.ENCONMAN.2022.116029.
[23] García-Mariaca A, Llera-Sastresa E. Techno-economic assessment for the practicability of on-board CO_2 capture in ICE vehicles. Appl Energy 2024;376:124167. https://doi.org/10.1016/j.apenergy.2024.124167.
[24] García-Mariaca A, Llera-Sastresa E. Energy and economic analysis feasibility of CO_2 capture on a natural gas internal combustion engine. Greenhouse Gases Sci Technol 2022. https://doi.org/10.1002/GHG.2176.
[25] García-Mariaca A, Perpiñán J, Carreño Sayago UF. Techno-economic analysis of integrating an on-board CCS system and a PtG technology in a heavy vehicle fleet. J CO2 Util 2025;93:103046. https://doi.org/10.1016/j.jcou.2025.103046.
[26] Sullivan JM, Sivak M. Carbon capture in vehicles: a review of general support, available mechanisms, and consumer acceptance issues. 2012.
[27] Raganati F, Ammendola P. CO_2 post-combustion capture: a critical review of current technologies and future directions. Energy Fuel 2024;38:13858–905. https://doi.org/10.1021/acs.energyfuels.4c02513.
[28] Wang K, Chi Y, Liang H, Jing Z, Li Z, Ma R, et al. Carbon emission monitoring and control technology for ships: a review. Mar Pollut Bull 2025;219:118219. https://doi.org/10.1016/j.marpolbul.2025.118219.
[29] Pancione E, Erto A, Di Natale F, Lancia A, Balsamo M. A comprehensive review of post-combustion CO_2 capture technologies for applications in the maritime sector: a focus on adsorbent materials. J CO2 Util 2024;89:102955. https://doi.org/10.1016/j.jcou.2024.102955.
[30] Zhang M, Perry Z, Park J, Zhou H-C. Stable benzimidazole-incorporated porous polymer network for carbon capture with high efficiency and low cost. Polymer (guildf) 2014;55:335–9. https://doi.org/10.1016/j.polymer.2013.09.029.
[31] Verdegaal WM, Wang K, Sculley JP, Wriedt M, Zhou HC. Evaluation of metal-organic frameworks and porous polymer networks for CO_2-capture applications. ChemSusChem 2016;9:636–43. https://doi.org/10.1002/cssc.201501464.
[32] Raganati F, Bellusci M, Leardi F, Varsano F, Ammendola P. CALF-20 obtained by mechanochemical synthesis for temperature swing adsorption CO_2 Capture: a thermodynamic and kinetic study. Chem Eng J 2025;506:159966. https://doi.org/10.1016/j.cej.2025.159966.
[33] Raganati F, Miccio F, Iervolino G, Papa E, Ammendola P. Waste-derived tuff for CO_2 capture: enhanced CO_2 adsorption performances by cation-exchange tailoring. J Ind Eng Chem 2024;138:153–64. https://doi.org/10.1016/j.jiec.2024.03.049.
[34] Gonzalez-Olmos R, Gutierrez-Ortega A, Sempere J, Nomen R. Zeolite versus carbon adsorbents in carbon capture: a comparison from an operational and life cycle perspective. J CO2 Util 2022;55:101791. https://doi.org/10.1016/j.jcou.2021.101791.
[35] Liang Z, Marshall M, Chaffee AL. CO $_2$ Adsorption-based separation by metal organic framework (Cu-BTC) versus zeolite (13X). Energy Fuel 2009;23:2785–9. https://doi.org/10.1021/ef800938e.
[36] Abdalla MA, Zentou H, Abdulhamid MA, Mohammed MG, Abdelnaby MM, Abdelaziz OY. A porous phenolic resin sorbent for enhanced CO_2 capture: synthesis, optimization, and techno-economic analysis. Fuel 2025;379:132961. https://doi.org/10.1016/j.fuel.2024.132961.
[37] Chen C, Park D-W, Ahn W-S. CO_2 capture using zeolite 13X prepared from bentonite. Appl Surf Sci 2014;292:63–7. https://doi.org/10.1016/j.apsusc.2013.11.064.
[38] Kwiatkowski M. An analysis of the textural properties of activated carbons obtained from biomass via the LBET, NLDFT and QSDFT methods. Sci Rep 2024;14:26472. https://doi.org/10.1038/s41598-024-76297-x.
[39] Plaza MG, García S, Rubiera F, Pis JJ, Pevida C. Post-combustion CO_2 capture with a commercial activated carbon: comparison of different regeneration strategies. Chem Eng J 2010;163:41–7. https://doi.org/10.1016/j.cej.2010.07.030.
[40] Drage TC, Blackman JM, Pevida C, Snape CE. Evaluation of activated carbon adsorbents for CO $_2$ capture in gasification. Energy Fuel 2009;23:2790–6. https://doi.org/10.1021/ef8010614.
[41] Bhati G, Dharanikota NPSK, Uppaluri RVS, Mandal B. Influence of cation exchange on the selective CO_2 adsorption performance of Zeolite-Y over CH_4 and N_2. Microporous Mesoporous Mater 2025;387:113537. https://doi.org/10.1016/j.micromeso.2025.113537.
[42] Fang H, Kulkarni A, Kamakoti P, Awati R, Ravikovitch PI, Sholl DS. Identification of High-CO $_2$ -capacity cationic zeolites by accurate computational screening. Chem Mater 2016;28:3887–96. https://doi.org/10.1021/acs.chemmater.6b01132.
[43] Serafin J, Dziejarski B. Activated carbons—preparation, characterization and their application in CO_2 capture: a review. Environ Sci Pollut Res 2023;31:40008–62. https://doi.org/10.1007/s11356-023-28023-9.

[44] Liu J, Sun X, Li N, Tan T, Zhang F, Sun M, et al. Effect of synthesis conditions on the properties of 13X zeolites for CO 2 adsorption. Environ Pollut Bioavailability 2024; 36. https://doi.org/10.1080/26395940.2024.2387683.
[45] Akpasi SO, Isa YM. Effect of operating variables on CO_2 adsorption capacity of activated carbon, kaolinite, and activated carbon – kaolinite composite adsorbent. Water-Energy Nexus 2022;5:21–8. https://doi.org/10.1016/j.wen.2022.08.001.
[46] Bell JG, Benham MJ, Thomas KM. Adsorption of carbon dioxide, water vapor, nitrogen, and sulfur dioxide on activated carbon for capture from flue gases: competitive adsorption and selectivity aspects. Energy Fuel 2021;35:8102–16. https://doi.org/10.1021/acs.energyfuels.1c00339.
[47] Wang Y, LeVan MD. Adsorption equilibrium of binary mixtures of carbon dioxide and water vapor on Zeolites 5A and 13X. J Chem Eng Data 2010;55:3189–95. https://doi.org/10.1021/je100053g.
[48] Shigaki N, Mogi Y, Haraoka T, Furuya E. Measurements and calculations of the equilibrium adsorption amounts of CO_2–N_2, CO–N_2, and CO_2–CO mixed gases on 13X zeolite. SN Appl Sci 2020;2:488. https://doi.org/10.1007/s42452-020-2298-y.
[49] Ma X, Albertsma J, Gabriels D, Horst R, Polat S, Snoeks C, et al. Carbon monoxide separation: past, present and future. Chem Soc Rev 2023;52:3741–77. https://doi.org/10.1039/D3CS00147D.
[50] Neathery JK, Rubel AM, Stencel JM. Uptake of NOX by activated carbons: bench-scale and pilot-plant testing. Carbon N Y 1997;35:1321–7. https://doi.org/10.1016/S0008-6223(97)00089-4.
[51] Deng H, Yi H, Tang X, Yu Q, Ning P, Yang L. Adsorption equilibrium for sulfur dioxide, nitric oxide, carbon dioxide, nitrogen on 13X and 5A zeolites. Chem Eng J 2012;188:77–85. https://doi.org/10.1016/j.cej.2012.02.026.
[52] Zhang D, Cheng W, Ma J, Li R. Influence of activated carbon in zeolite X/activated carbon composites on CH_4/N_2 adsorption separation ability. Adsorption 2016;22: 1129–35. https://doi.org/10.1007/s10450-016-9836-3.
[53] Valadi FM, Pasandideh-Nadamani M, Rezaee M, Torrik A, Mirzaie M, Torkian A. Competitive adsorption of CO_2, N_2, and CH_4 in coal-derived asphaltenes, a computational study. Sci Rep 2024;14:7664. https://doi.org/10.1038/s41598-024-58347-6.
[54] Stoeckli F, Centeno TA. On the determination of surface areas in activated carbons. Carbon N Y 2005;43:1184–90. https://doi.org/10.1016/j.carbon.2004.12.010.
[55] Li H, Guo H, Shen S. Low-energy-consumption CO_2 capture by liquid-solid phase change absorption using water-lean blends of amino acid salts and 2-alkoxyethanols. ACS Sustain Chem Eng 2020;8:12956–67. https://doi.org/10.1021/acssuschemeng.0c03525.
[56] Tian W, Ma K, Ji J, Tang S, Zhong S, Liu C, et al. Nonaqueous MEA/PEG200 absorbent with high efficiency and low energy consumption for CO_2 capture. Ind Eng Chem Res 2021;60:3871–80. https://doi.org/10.1021/acs.iecr.0c05294.
[57] Jiang N, Shen Y, Liu B, Zhang D, Tang Z, Li G, et al. CO_2 capture from dry flue gas by means of VPSA, TSA and TVSA. J CO2 Util 2020;35:153–68. https://doi.org/10.1016/j.jcou.2019.09.012.
[58] Mondino G, Spjelkavik AI, Didriksen T, Krishnamurthy S, Stensrød RE, Grande CA, et al. Production of MOF adsorbent spheres and comparison of their performance with zeolite 13X in a moving-bed TSA process for postcombustion CO_2 capture. Ind Eng Chem Res 2020;59:7198–211. https://doi.org/10.1021/acs.iecr.9b06387.